Acta Cryst E CRYSTALLOGRAPHIC COMMUNICATIONS

ISSN 2056-9890

Crystal structure and Hirshfeld surface analysis of new polymorph of racemic 2-phenylbutyramide

Sergei Rigin,[a]* Beatrice Armijo,[a] Arcadius V. Krivoshein,[b] Marina Fonari[c] and Tatiana Timofeeva[a]

[a]Department of Chemistry, New Mexico Highlands University, Las Vegas, New Mexico, 87701, USA, [b]Department of Physical & Applied Sciences, University of Houston – Clear Lake, 2700 Bay Area Boulevard, Houston, TX 77058, USA, and [c]Institute of Applied Physics, Academy str., 5 MD2028, Chisinau, Moldova. *Correspondence e-mail: rigindale@gmail.com

Received 29 April 2019
Accepted 14 May 2019

Edited by A. V. Yatsenko, Moscow State University, Russia

Keywords: crystal structure; racemate; 2-phenylbutyramide; hydrogen bonds; Hirshfeld surface analysis.

CCDC reference: 1916098

Supporting information: this article has supporting information at journals.iucr.org/e

A new polymorph of the title compound, $C_{10}H_{13}NO$, was obtained by recrystallization of the commercial product from a water/ethanol mixture (1:1 *v*/*v*). Crystals of the previously reported racemic and homochiral forms of 2-phenylbutyramide were grown from water–acetonitrile solution in 1:1 volume ratio [Khrustalev *et al.* (2014). *Cryst. Growth Des.* **14**, 3360–3369]. While the previously reported racemic and enantiopure forms of the title compound adopt very similar supramolecular structures (hydrogen-bonded ribbons), the new racemic polymorph is stabilized by a single N—H···O hydrogen bond that links molecules into chains along the *c*-axis direction with an antiparallel (centrosymmetric) packing in the crystal. Hirshfeld molecular surface analysis was employed to compare the intermolecular interactions in the polymorphs of the title compound.

1. Chemical context

Many drugs exist in several polymorphic modifications (Bernstein, 2011; Brittain, 2009). For example, a second polymorph, II, was reported (Vishweshwar *et al.*, 2005) in 2005 for aspirin, one of the most widely consumed medications; this was similar in structure to the original form I (Wheatley, 1964) and was widely discussed (Bond *et al.*, 2007, 2011). The third ambient polymorph of aspirin, crystallized from the melt, was described recently using a combination of X-ray powder diffraction analysis and crystal structure prediction algorithms (Shtukenberg *et al.*, 2017). Paracetamol, one of the most frequently used antipyretic and analgesic drugs, is known in three crystal modifications: a monoclinic (form I) (Haisa *et al.*, 1976), an orthorhombic (form II) (Haisa *et al.*, 1974), and an unstable phase (form III), which can only be stabilized under certain conditions (Burger & Ramberger, 1979). The non-steroidal anti-inflammatory drug mefenamic acid is known to exist as dimorphs (I and II) and a metastable polymorph obtained during co-crystallization experiments (Seetha-Lekshmi & Guru Row, 2012). The existence of three different polymorphic forms has been reported for anhydrous carbamazepine, an anticonvulsant drug (Rustichelli *et al.*, 2000). We previously reported (Khrustalev *et al.*, 2014) two polymorphs of α-methyl-α-phenylsuccinimide (3-methyl-3-phenylpyrrolidine-2,5-dione), the *N*-demethylated metabolite of the anticonvulsant methsuximide. Herein, we report on the crystal structure and the Hirshfeld surface analysis of a new polymorph of the title compound, obtained by recrystallization of

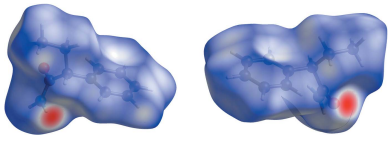

the commercial product (Alfa Aesar, stock No. A18501) from a water–ethanol (1:1) solution. Crystals of the previously reported racemic and homochiral forms of 2-phenylbutyramide were grown from water–acetonitrile solution in a 1:1 volume ratio (Khrustalev *et al.*, 2014).

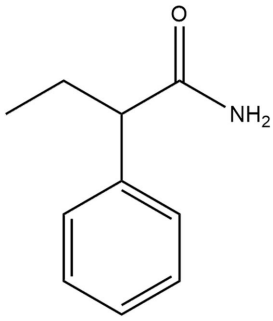

2. Structural commentary

A view of the molecule of the new polymorph (henceforth referred to as *rac*-2) is illustrated in Fig. 1*a*. In the molecule, the rotation of the amide group around the C7—C10 bond is characterized by an N1—C10—C7—C8 torsion angle of −141.14 (9)°, thus corresponding in conformation to the previously reported polymorph (further notated as *rac*-1, space group *C*2/*c*), where the torsion angle is −130.06 (9)°, and one of two conformers in the *R*-enantiomer [space group *P*1, torsion angle = −144.08 (13)°; Khrustalev *et al.*, 2014). The overlay diagram for the two racemic forms shown in Fig. 1*b* shows the almost perfect fit (r.m.s. deviation = 0.263 Å). The bond lengths in the molecule are in line with those of reported analogues (CSD version 5.40, last update November 2018; Groom *et al.*, 2016).

3. Supramolecular features

Molecule of the title compound contain one amino group as a potential double hydrogen-bond donor and one carbonyl group capable of acting as a multiple hydrogen-bond acceptor. Contrary to the previously reported *rac*-1 and two enantiomeric forms (Khrustalev *et al.*, 2014), where the amino group acted as double hydrogen-bond donor while the carbonyl oxygen atom acted as a double hydrogen-bond acceptor being involved in two N–H···O hydrogen bonds leading to the formation of supramolecular ribbons, in *rac*-2 only one hydrogen atom of the amino group is involved in a single N—H···O hydrogen bond (Table 1). This hydrogen bond links molecules related by the glide plane into chains along the *c*-axis direction (Fig. 2). The packing of the chains obeys inversion symmetry with only van der Waals contacts between the chains (Fig. 3). In spite of the fewer number of strong directed intermolecular interactions in the crystal, the structure of *rac*-2 is characterized by a more effective crystal packing of the single chains, compared to the packing of ribbons in *rac*-1 and in the enantiomers, which follows from the higher value of the crystal density (calculated as 1.227 g cm^{-3}; Table 2) compared with values of 1.160 g cm^{-3}

Table 1
Hydrogen-bond geometry (Å, °).

D—H···*A*	*D*—H	H···*A*	*D*···*A*	*D*—H···*A*
N1—H1*B*···O1^{i}	0.895 (15)	2.071 (15)	2.9533 (13)	168.4 (13)

Symmetry code: (i) $x, -y+\frac{1}{2}, z+\frac{1}{2}$.

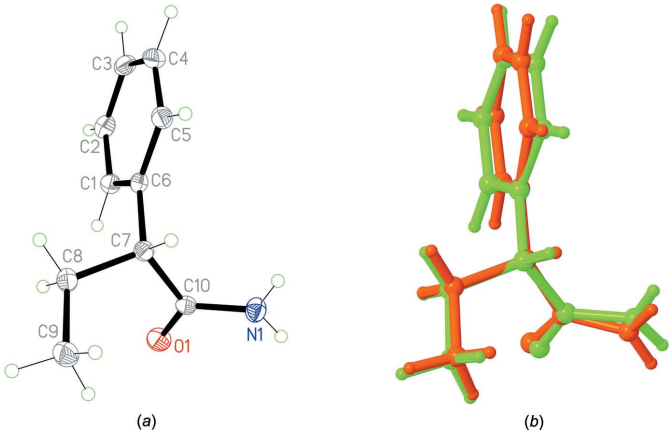

Figure 1
(*a*) View of the molecular structure of the title *rac*-2 polymorph with the atom labelling. Displacement ellipsoids are drawn at the 50% probability level. (*b*) Superposition of the *rac*-1 (red) and *rac*-2 (green) polymorphs.

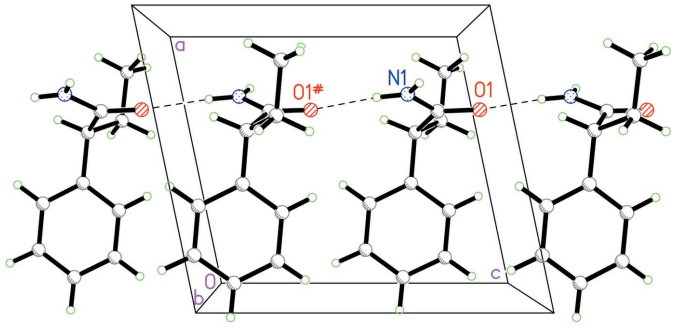

Figure 2
View of a hydrogen-bonded chain.

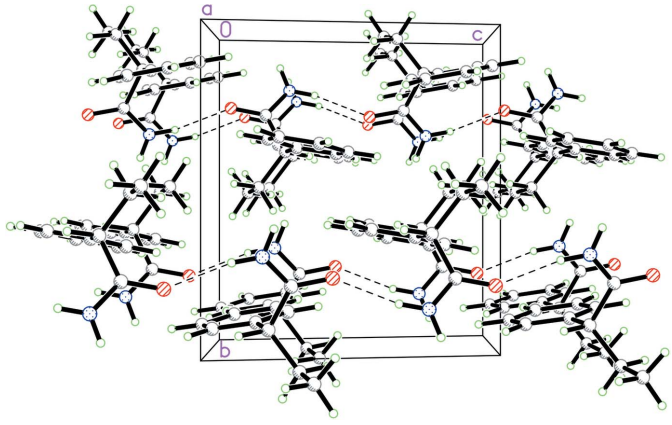

Figure 3
The crystal packing of the *rac*-2 polymorph.

Table 2
Crystal lattice energies (kJ mol^{-1}) for racemic 2-phenylbutyramide polymorphs computed using *AA-CLP* software.

Polymorph	$E_{electrostatic}$	$E_{polarization}$	$E_{dispersion}$	$E_{exchange\text{-}repulsion}$	E_{total}	Crystal density (g cm^{-3})
rac-1	−35.6[a]	−27.6[a]	−100.4[a]	55.0[a]	−108.6[a]	1.160[b]
rac-2	−33.9	−28.3	−107.9	53.8	−116.3	1.227

Notes: [a]from Krivoshein *et al.* (2018); [b]from Khrustalev *et al.* (2014).

for *rac*-1 and 1.188 g cm^{-3} and 1.189 g cm^{-3} for the *R*- and *S*-enantiomers (Khrustalev *et al.*, 2014).

4. Hirshfeld surface analysis and calculation of crystal lattice energies

Crystal Explorer (Wolff *et al.*, 2012) was used to generate the Hirshfeld surfaces (Hirshfeld, 1977). The total d_{norm} surfaces for polymorphs *rac*-2 and *rac*-1 are shown in Figs. 4 and 5, respectively, in which the red spots correspond to the most significant N—H···O interactions in the crystal (Table 1). The surface diagram unambiguously shows that there are fewer active binding sites in *rac*-2 in comparison to *rac*-1. The two-dimensional fingerprint plots from the Hirshfeld surface analysis (Spackman & Jayatilaka, 2009) allows the intermolecular interactions to be analysed in detail and for even rather subtle differences between polymorphic systems to be quantified (Bernstein, 2011). The two-dimensional fingerprint plots for *rac-2* and *rac-1* are shown in Figs. 6 and 7, respectively. They clearly indicate the different distribution of interactions for a single molecule in the two structures. Decomposition of the full fingerprint plot for *rac*-2 shows five principle types of interactions that include H···H, H···C/C···H, H···O/O···H, H···N/N···H, and C···O/O···C contacts in decreasing order (Fig. 6). For the *rac*-1 polymorph, the set includes only four types of interactions, *viz*. H···H, H···C/C···H, H···O/O···H and H···N/N···H contacts (Fig. 7). The predominant interactions in both cases are H···H, constituting 65.7% in *rac*-2 and 67.3% in *rac*-1. With a significantly less contribution, the next most important interactions are H···C/C···H, contributing 19.6% in both cases, and being slightly asymmetric in shape in favour of (internal)C···H(external) contacts for both polymorphs. The

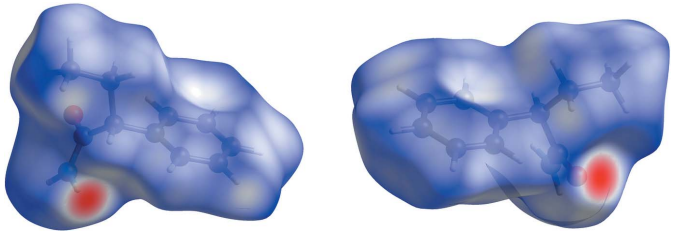

Figure 4
Hirshfeld surface for the *rac*-2 polymorph plotted over d_{norm} in the range −0.4994 to 1.0567 a.u.

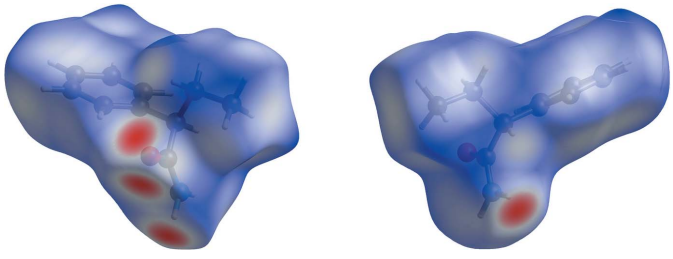

Figure 5
Hirshfeld surface for the *rac*-1 polymorph plotted over d_{norm} in the range −0.5239 to 1.3882 a.u.

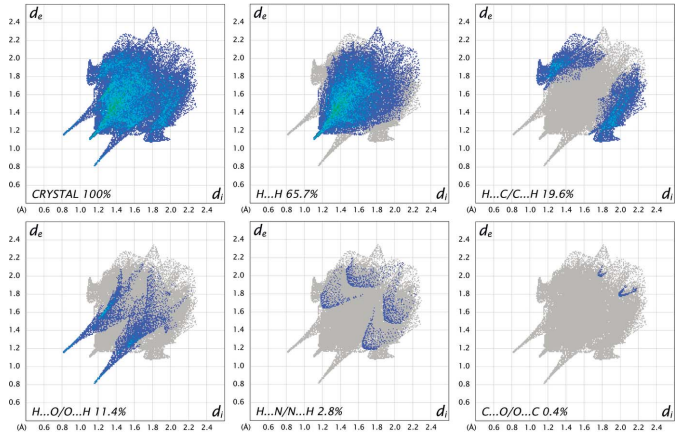

Figure 6
The full two-dimensional fingerprint plots for the *rac*-2 polymorph, showing all interactions, and delineated into H···H, H···C/C···H, H···O/O···H, H···N/N···H, C···O/O···C interactions. The d_i and d_e values are the closest internal and external distances (in Å) from given points on the Hirshfeld surface.

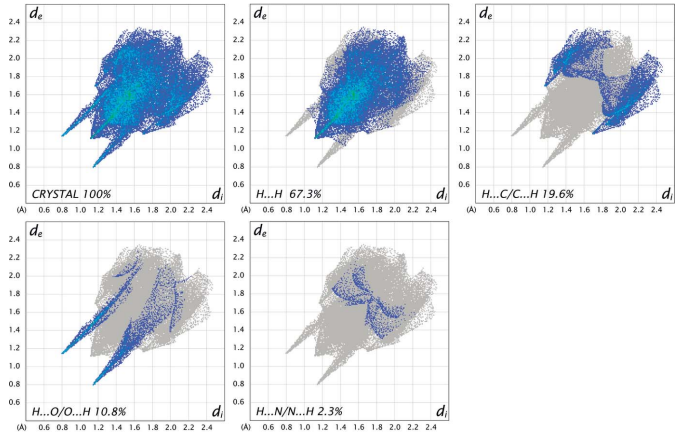

Figure 7
The full two-dimensional fingerprint plots for the *rac*-1 polymorph, showing all interactions, and delineated into H···H, H···C/C···H, H···O/O···H and H···N/N···H interactions. The d_i and d_e values are the closest internal and external distances (in Å) from given points on the Hirshfeld surface.

Table 3
Experimental details.

Crystal data	
Chemical formula	$C_{10}H_{13}NO$
M_r	163.21
Crystal system, space group	Monoclinic, $P2_1/c$
Temperature (K)	100
a, b, c (Å)	8.575 (2), 10.746 (3), 9.798 (3)
β (°)	101.811 (3)
V (Å^3)	883.8 (4)
Z	4
Radiation type	Mo $K\alpha$
μ (mm^{-1})	0.08
Crystal size (mm)	0.15 × 0.1 × 0.1
Data collection	
Diffractometer	Bruker APEXII CCD
Absorption correction	Multi-scan (*SADABS*; Bruker, 2004)
T_{min}, T_{max}	0.674, 0.746
No. of measured, independent and observed [$I > 2\sigma(I)$] reflections	9961, 2240, 1914
R_{int}	0.038
(sin $\theta/\lambda)_{max}$ (Å^{-1})	0.671
Refinement	
$R[F^2 > 2\sigma(F^2)]$, $wR(F^2)$, S	0.040, 0.110, 1.08
No. of reflections	2240
No. of parameters	161
H-atom treatment	All H-atom parameters refined
$\Delta\rho_{max}$, $\Delta\rho_{min}$ (e Å^{-3})	0.31, −0.27

Computer programs: *APEX2* and *SAINT* (Bruker, 2004), *SHELXT* (Sheldrick, 2015*a*), *SHELXL* (Sheldrick, 2015*b*)and *OLEX2* (Dolomanov *et al.*, 2009).

directed H···O/O···H contacts constitute 11.4% for *rac*-2 and 10.8% for *rac*-1, with slight a asymmetry in favour of (internal)O···H(external) contacts for both polymorphs.

The Hirshfeld surface analysis confirms the decisive role of H-contacts that include hydrogen bonding and van der Waals interactions in the crystal packing. The crystal-lattice energies (Table 2) were calculated from the atomic coordinates obtained in the single-crystal X-ray diffraction experiments using the atom–atom force field with subdivision of the interaction energies into Coulombic, polarization, London dispersion, and Pauli repulsion components (*AA-CLP*; Gavezzotti, 2011, 2013) implemented in the *CLP-PIXEL* computer program package (version 3.0, available from www.angelogavezzotti.it). These show that the *rac*-2 polymorph is more stable in terms of two criteria: total crystal energy and crystal density.

5. Database survey

The Cambridge Structural Database (CSD version 5.40, last update November 2018; Groom *et al.*, 2016) includes crystallographic data for the *R*- and *S*-enantiomers of 2-phenylbutyramide (VOQGUF and VOQHAM, space group *P*1; Khrustalev *et al.*, 2014) and the racemic form (VOQHEQ, space group *C*2/*c*; Khrustalev *et al.*, 2014). As mentioned above, the conformations of two *rac*-polymorphs are quite similar, while the crystal packing differs significantly with more efficient crystal packing for the *rac*-2 polymorph reported here.

6. Crystallization

Crystals were obtain by the slow evaporation approach. 0.5 g of 2-phenylbutyramide (Alfa Aesar, stock No. A18501) were dissolved with extensive vortexing in 3 mL of a water/ethanol mixture (1:1 *v*/*v*) and left at room temperature (293–295 K) for six weeks. Block-shaped crystals formed on the walls of the vessel.

7. Refinement

Crystal data, data collection and structure refinement details are summarized in Table 3.

Funding information

Funding for this research was provided by: NSF DMR 1523611 (PREM) and Welch Foundation (Departmental Grant; award No. BC-0022) .

References

Bernstein, J. (2011). *Cryst. Growth Des.* **11**, 632–650.
Bond, A. D., Boese, R. & Desiraju, G. R. (2007). *Angew. Chem. Int. Ed.* **46**, 618–622.
Bond, A. D., Solanko, K. A., Parsons, S., Redder, S. & Boese, R. (2011). *CrystEngComm*, **13**, 399–401.
Brittain, H. G. (2009). *Polymorphism in pharmaceutical solids.* Informa, Healthcare. NY.
Bruker (2004). *SAINT*, *APEX2* and *SADABS*. Bruker AXS Inc., Madison, Wisconsin, USA.
Burger, A. & Ramberger, R. (1979). *Mikrochim. Acta*, **72**, 273–316.
Dolomanov, O. V., Bourhis, L. J., Gildea, R. J., Howard, J. A. K. & Puschmann, H. (2009). *J. Appl. Cryst.* **42**, 339–341.
Gavezzotti, A. (2011). *New J. Chem.* **35**, 1360–1368.
Gavezzotti, A. (2013). *New J. Chem.* **37**, 2110–2119.
Groom, C. R., Bruno, I. J., Lightfoot, M. P. & Ward, S. C. (2016). *Acta Cryst.* B**72**, 171–179.
Haisa, M., Kashino, S., Kawai, R. & Maeda, H. (1976). *Acta Cryst.* B**32**, 1283–1285.
Haisa, M., Kashino, S. & Maeda, H. (1974). *Acta Cryst.* B**30**, 2510–2512.
Hirshfeld, F. L. (1977). *Theor. Chim. Acta*, **44**, 129–138.
Khrustalev, V. N., Sandhu, B., Bentum, S., Fonari, A., Krivoshein, A. V. & Timofeeva, T. V. (2014). *Cryst. Growth Des.* **14**, 3360–3369.
Krivoshein, A. V., Lindeman, S. V., Bentum, S., Averkiev, B. B., Sena, V. & Timofeeva, T. V. (2018). *Z. Kristallogr. Cryst. Mat.* **233**, 781–793.
Rustichelli, C., Gamberini, G., Ferioli, V., Gamberini, M. C., Ficarra, R. & Tommasini, S. (2000). *J. Pharm. Biomed. Anal.* **23**, 41–54.
SeethaLekshmi, S. & Guru Row, T. N. (2012). *Cryst. Growth Des.* **12**, 4283–4289.
Sheldrick, G. M. (2015*a*). *Acta Cryst.* A**71**, 3–8.
Sheldrick, G. M. (2015*b*). *Acta Cryst.* C**71**, 3–8.
Shtukenberg, A. G., Hu, C. T., Zhu, Q., Schmidt, M. U., Xu, W., Tan, M. & Kahr, B. (2017). *Cryst. Growth Des.* **17**, 3562–3566.
Spackman, M. A. & Jayatilaka, D. (2009). *CrystEngComm*, **11**, 19–32.
Vishweshwar, P., McMahon, J. A., Oliveira, M., Peterson, M. L. & Zaworotko, M. J. (2005). *J. Am. Chem. Soc.* **127**, 16802–16803.
Wheatley, P. J. (1964). *J. Chem. Soc.* pp. 6036–6048.
Wolff, S. K., Grimwood, D. J., McKinnon, J. J., Turner, M. J., Jayatilaka, D. & Spackman, M. A. (2012). *Crystal Explorer*. University of Western Australia, Australia.

supporting information

Acta Cryst. (2019). E**75**, 826-829 [https://doi.org/10.1107/S2056989019007011]

Crystal structure and Hirshfeld surface analysis of new polymorph of racemic 2-phenylbutyramide

Sergei Rigin, Beatrice Armijo, Arcadius V. Krivoshein, Marina Fonari and Tatiana Timofeeva

Computing details

Data collection: *SAINT* (Bruker, 2004); cell refinement: *APEX2* (Bruker, 2004); data reduction: *SAINT* (Bruker, 2004); program(s) used to solve structure: SHELXT (Sheldrick, 2015a); program(s) used to refine structure: *SHELXL* (Sheldrick, 2015b); molecular graphics: *OLEX2* (Dolomanov *et al.*, 2009); software used to prepare material for publication: *OLEX2* (Dolomanov *et al.*, 2009).

2-Phenylbutyramide

Crystal data

$C_{10}H_{13}NO$
$M_r = 163.21$
Monoclinic, $P2_1/c$
$a = 8.575$ (2) Å
$b = 10.746$ (3) Å
$c = 9.798$ (3) Å
$\beta = 101.811$ (3)°
$V = 883.8$ (4) Å^3
$Z = 4$
$F(000) = 352$
$D_x = 1.227$ Mg m^{-3}
Mo $K\alpha$ radiation, $\lambda = 0.71073$ Å
Cell parameters from 3598 reflections
$\theta = 2.4$–$30.1°$
$\mu = 0.08$ mm^{-1}
$T = 100$ K
Block, colourless
0.15 × 0.1 × 0.1 mm

Data collection

Bruker APEXII CCD diffractometer
φ and ω scans
Absorption correction: multi-scan (SADABS; Bruker, 2004)
$T_{min} = 0.674$, $T_{max} = 0.746$
9961 measured reflections
2240 independent reflections
1914 reflections with $I > 2\sigma(I)$
$R_{int} = 0.038$
$\theta_{max} = 28.5°$, $\theta_{min} = 2.4°$
$h = -11 \rightarrow 10$
$k = -14 \rightarrow 14$
$l = -13 \rightarrow 13$

Refinement

Refinement on F^2
Least-squares matrix: full
$R[F^2 > 2\sigma(F^2)] = 0.040$
$wR(F^2) = 0.110$
$S = 1.08$
2240 reflections
161 parameters
0 restraints
Primary atom site location: dual
Hydrogen site location: difference Fourier map
All H-atom parameters refined
$w = 1/[\sigma^2(F_o^2) + (0.0614P)^2 + 0.1474P]$ where $P = (F_o^2 + 2F_c^2)/3$
$(\Delta/\sigma)_{max} < 0.001$
$\Delta\rho_{max} = 0.31$ e Å^{-3}
$\Delta\rho_{min} = -0.27$ e Å^{-3}

Special details

Geometry. All esds (except the esd in the dihedral angle between two l.s. planes) are estimated using the full covariance matrix. The cell esds are taken into account individually in the estimation of esds in distances, angles and torsion angles; correlations between esds in cell parameters are only used when they are defined by crystal symmetry. An approximate (isotropic) treatment of cell esds is used for estimating esds involving l.s. planes.

Fractional atomic coordinates and isotropic or equivalent isotropic displacement parameters (Å²)

	x	*y*	*z*	U_{iso}*/U_{eq}
O1	0.32919 (9)	0.23775 (7)	0.06137 (7)	0.0216 (2)
N1	0.27946 (11)	0.17768 (8)	0.26886 (9)	0.0192 (2)
H1A	0.2469 (17)	0.1033 (15)	0.2342 (15)	0.031 (4)*
H1B	0.2895 (17)	0.1927 (14)	0.3601 (15)	0.028 (3)*
C1	0.68011 (12)	0.34374 (9)	0.20614 (10)	0.0179 (2)
H1	0.6296 (16)	0.3276 (12)	0.1099 (14)	0.021 (3)*
C2	0.84492 (13)	0.33963 (10)	0.24848 (11)	0.0206 (2)
H2	0.9097 (17)	0.3192 (13)	0.1809 (14)	0.027 (3)*
C3	0.91672 (13)	0.36033 (10)	0.38704 (11)	0.0217 (2)
H3	1.0322 (19)	0.3568 (14)	0.4177 (15)	0.035 (4)*
C4	0.82161 (13)	0.38440 (10)	0.48320 (11)	0.0219 (2)
H4	0.8698 (17)	0.3979 (13)	0.5822 (15)	0.027 (3)*
C5	0.65680 (13)	0.38737 (9)	0.44137 (10)	0.0184 (2)
H5	0.5908 (15)	0.4038 (12)	0.5099 (13)	0.017 (3)*
C6	0.58384 (12)	0.36770 (8)	0.30233 (10)	0.0151 (2)
C7	0.40388 (12)	0.37876 (9)	0.25694 (10)	0.0150 (2)
H7	0.3586 (15)	0.3913 (12)	0.3424 (13)	0.019 (3)*
C8	0.35882 (12)	0.49138 (9)	0.16087 (11)	0.0189 (2)
H8A	0.4084 (18)	0.5661 (13)	0.2142 (15)	0.030 (4)*
H8B	0.4098 (16)	0.4803 (12)	0.0771 (14)	0.024 (3)*
C9	0.18019 (13)	0.50974 (11)	0.11476 (12)	0.0226 (2)
H9A	0.1318 (18)	0.4394 (14)	0.0522 (15)	0.033 (4)*
H9B	0.1575 (19)	0.5862 (15)	0.0573 (16)	0.039 (4)*
H9C	0.1253 (18)	0.5153 (14)	0.1957 (16)	0.034 (4)*
C10	0.33405 (11)	0.25883 (9)	0.18573 (10)	0.0148 (2)

Atomic displacement parameters (Å²)

	U^{11}	U^{22}	U^{33}	U^{12}	U^{13}	U^{23}
O1	0.0261 (4)	0.0250 (4)	0.0141 (4)	−0.0021 (3)	0.0046 (3)	−0.0035 (3)
N1	0.0241 (5)	0.0158 (4)	0.0184 (4)	−0.0028 (3)	0.0060 (3)	−0.0006 (3)
C1	0.0198 (5)	0.0181 (5)	0.0155 (4)	−0.0020 (4)	0.0026 (4)	−0.0003 (3)
C2	0.0202 (5)	0.0185 (5)	0.0244 (5)	−0.0016 (4)	0.0073 (4)	−0.0004 (4)
C3	0.0168 (5)	0.0182 (5)	0.0279 (5)	−0.0025 (4)	−0.0004 (4)	0.0011 (4)
C4	0.0259 (6)	0.0191 (5)	0.0177 (5)	−0.0025 (4)	−0.0025 (4)	−0.0003 (4)
C5	0.0227 (5)	0.0160 (5)	0.0162 (5)	−0.0006 (4)	0.0034 (4)	−0.0003 (3)
C6	0.0167 (5)	0.0118 (4)	0.0163 (4)	−0.0012 (3)	0.0022 (3)	0.0010 (3)
C7	0.0163 (5)	0.0159 (5)	0.0129 (4)	−0.0007 (3)	0.0035 (3)	−0.0002 (3)
C8	0.0187 (5)	0.0176 (5)	0.0202 (5)	−0.0003 (4)	0.0036 (4)	0.0036 (4)

C9	0.0196 (5)	0.0231 (5)	0.0244 (5)	0.0031 (4)	0.0028 (4)	0.0036 (4)
C10	0.0131 (4)	0.0158 (4)	0.0150 (4)	0.0012 (3)	0.0020 (3)	−0.0003 (3)

Geometric parameters (Å, º)

O1—C10	1.2316 (12)	C5—H5	0.979 (12)
N1—H1A	0.890 (16)	C5—C6	1.3940 (14)
N1—H1B	0.895 (15)	C6—C7	1.5206 (14)
N1—C10	1.3414 (13)	C7—H7	1.002 (12)
C1—H1	0.970 (13)	C7—C8	1.5333 (14)
C1—C2	1.3898 (15)	C7—C10	1.5282 (13)
C1—C6	1.3982 (14)	C8—H8A	1.004 (14)
C2—H2	0.973 (14)	C8—H8B	1.013 (13)
C2—C3	1.3891 (15)	C8—C9	1.5187 (15)
C3—H3	0.975 (16)	C9—H9A	1.007 (15)
C3—C4	1.3909 (16)	C9—H9B	0.992 (16)
C4—H4	0.984 (14)	C9—H9C	1.004 (15)
C4—C5	1.3890 (15)		
H1A—N1—H1B	120.1 (13)	C6—C7—H7	108.0 (7)
C10—N1—H1A	118.2 (9)	C6—C7—C8	110.76 (8)
C10—N1—H1B	121.0 (9)	C6—C7—C10	110.30 (8)
C2—C1—H1	120.6 (8)	C8—C7—H7	108.4 (7)
C2—C1—C6	120.62 (9)	C10—C7—H7	108.2 (7)
C6—C1—H1	118.8 (8)	C10—C7—C8	111.06 (8)
C1—C2—H2	119.4 (8)	C7—C8—H8A	106.5 (8)
C3—C2—C1	120.46 (10)	C7—C8—H8B	107.9 (8)
C3—C2—H2	120.1 (8)	H8A—C8—H8B	108.0 (11)
C2—C3—H3	120.9 (9)	C9—C8—C7	113.41 (8)
C2—C3—C4	119.20 (10)	C9—C8—H8A	110.2 (8)
C4—C3—H3	119.9 (9)	C9—C8—H8B	110.5 (8)
C3—C4—H4	120.6 (8)	C8—C9—H9A	110.4 (8)
C5—C4—C3	120.45 (9)	C8—C9—H9B	110.2 (9)
C5—C4—H4	119.0 (8)	C8—C9—H9C	112.4 (9)
C4—C5—H5	119.9 (7)	H9A—C9—H9B	105.6 (12)
C4—C5—C6	120.73 (9)	H9A—C9—H9C	108.9 (12)
C6—C5—H5	119.4 (7)	H9B—C9—H9C	109.2 (12)
C1—C6—C7	121.41 (9)	O1—C10—N1	122.40 (9)
C5—C6—C1	118.55 (9)	O1—C10—C7	122.52 (9)
C5—C6—C7	119.98 (9)	N1—C10—C7	115.07 (8)
C1—C2—C3—C4	0.44 (16)	C5—C6—C7—C8	112.46 (10)
C1—C6—C7—C8	−64.48 (12)	C5—C6—C7—C10	−124.17 (9)
C1—C6—C7—C10	58.89 (11)	C6—C1—C2—C3	−0.55 (16)
C2—C1—C6—C5	0.03 (15)	C6—C7—C8—C9	−178.47 (8)
C2—C1—C6—C7	177.01 (9)	C6—C7—C10—O1	−83.85 (11)
C2—C3—C4—C5	0.18 (15)	C6—C7—C10—N1	95.67 (10)
C3—C4—C5—C6	−0.70 (15)	C8—C7—C10—O1	39.34 (13)

C4—C5—C6—C1	0.59 (15)	C8—C7—C10—N1	−141.14 (9)
C4—C5—C6—C7	−176.43 (9)	C10—C7—C8—C9	58.60 (11)

Hydrogen-bond geometry (Å, º)

D—H···*A*	*D*—H	H···*A*	*D*···*A*	*D*—H···*A*
N1—H1*B*···O1^{i}	0.895 (15)	2.071 (15)	2.9533 (13)	168.4 (13)

Symmetry code: (i) *x*, −*y*+1/2, *z*+1/2.